

Effect of sintering temperature and porosity on electro-deoxidation of calcium titanate in CaCl₂-NaCl molten salt

Guoli Zhao, Ying Xu, Yanqing Cai*

College of Materials Science and Engineering, North China University of Science and Technology, Hebei, Tangshan 063210, China

*E-mail: caiyanning126@126.com

Received: 5 November 2021 / Accepted: 17 December 2021 / Published: 5 January 2022

The performance of cathodes has an important influence on the degree of deoxidation when preparing titanium via a molten salt electro-deoxidation process. In this study, CaTiO₃ was used as a cathode to investigate the influence of sintering temperature on the degree of electro-deoxidation. The results show that increasing the sintering temperature from 900 °C to 1200 °C can effectively improve the conductivity of a CaTiO₃ cathode, which is conducive to electron migration. However, a high temperature (1300°C) leads to excessive grain growth, increasing the solid phase transport distance for O²⁻, which is not conducive to deep reduction of the cathode. When sintered at 1200°C, the CaTiO₃ cathode shows the most in-depth deoxidation, which is suitable for electro-deoxidation of the precursor to prepare titanium. In addition, the effect of porosity on the degree of deoxidation was also studied. When the NH₄HCO₃ content increases from 2% to 10%, the porosity is increased, which leads to a decrease in the mechanical strength of the cathode, and a part of the cathode becomes detached from the matrix during the electrolysis process, leading to failure of the reduction reaction. Moreover, a considerable amount of unreacted CaTiO₃ is present in the cathode product with 10 wt.% NH₄HCO₃ because the cathode with high porosity produces cracks in the electrolytic process. By comparing the deoxidation effect before and after adding 2% NH₄HCO₃ under optimal conditions, CaTiO₃ cathodes sintered at 1200°C without NH₄HCO₃ were found to be thoroughly electrolysed, with the purity of the titanium obtained reaching 97.65%.

Keywords: Molten salt electro-deoxidation, sintering temperature, porosity, titanium.

1. INTRODUCTION

Titanium and its alloys are widely used in various fields because of their high strength, good corrosion resistance, and high heat resistance. The molten salt electro-deoxidation (FFC) process is a direct process used to prepare pure metal titanium from titanium oxide[1,2] and has been studied for nearly 20 years. The main mechanism for this process involves TiO₂ ionization by O²⁻ under an applied electric potential that is lower than the decomposition potential of the molten salt but higher than the

reduction potential of TiO_2 . The O^{2-} ions enter the molten salt and discharge after reaching the graphite anode to generate CO or CO_2 , thus leaving titanium metal at the cathode. Because the FFC method uses TiO_2 as a cathode precursor system to prepare titanium metal, the current efficiency is low, the side reactions of TiO_2 in molten salts result in excessive oxygen content in the product. Therefore, this method has not been industrialized yet.

In recent years, quickly obtaining the target product in a short time has become a research hotspot. In fact, in the electro-deoxidation process, the experimental speed is affected by many factors, such as the reaction process, molten salt selection, cathode and anode performance. The most important of these factors is the performance of the cathode and anode as the main reactants. Fray[3] compared experimental speeds using graphite and nonconsumable oxide-based anodes. A SnO_2 -based anode can increase the speed at which the target product is obtained and does not produce carbon pollution. However, it leads to the formation of a CaSnO_3 insulating layer during the experiment[4]. When conductive titanium carbide is selected for the anode, a CaTiO_3 insulating layer is formed on the anode surface[5]. In recent years, CaRuO_3 has been used as an inert electrode material[6]. Jiao[7] showed that CaRuO_3 has good electrical conductivity. After a 150 h experiment, the CaRuO_3 anode shows no obvious corrosion phenomenon and can produce oxygen on its surface without polluting the melt. However, Ru is an extremely expensive element, and the preparation process for the CaRuO_3 anode is very complicated. Therefore, improving the cathode performance to perfect the experimental speed is a relatively simple method.

In terms of improving the cathode performance, the sintering temperature for the cathode plays an important role in the degree of deoxidation. By controlling the sintering parameters for the cathode, one can expect to improve the conductivity of the cathode, which directly affects the speed of electron transmission. Xu[8] showed that the conductivity of a cathode increases with increasing sintering temperature, and when the temperature is increased, a liquid phase is formed in the local area of the cathode, which makes the cathode denser and improves the connectivity and contact resistance between the particles. Second, when the temperature increases, the stronger polarization of the crystal will enhance the transmission of electrons. The main reason for this is that the original crystal vibrates strongly at high temperature, and some O atoms tend to break away from the original crystal, making the crystal itself an anoxic structure, that is, one that contains oxygen vacancies. Under the action of electrons, the existence of oxygen vacancies in the cathode sheet can promote the mutual transfer of oxygen atoms in each crystal cell to achieve electron transfer. Therefore, a high temperature can enhance the conductivity of some oxides due to the formation of oxygen vacancy structures. In this study, the influence of sintering temperature on the degree of electro-deoxidation was also investigated to explore the relationship between the conductivity of a cathode and its sintering temperature.[9]

Chen[10] attributed the oxygen removal rate in metal oxides to the small number of three-phase boundaries. The electro-deoxidation of metal oxide in molten salt is carried out through the metal wire/oxide/molten salt three-phase reaction interface (3PI). When the metal oxide is reduced to metal, 3PI becomes a metal product/unreacted oxide/molten salt, and 3PI migrates from the outside to the inside until the whole oxide cathode becomes a metal. Increasing the porosity of the cathode precursor can increase the reaction area of 3PI, thus improving the efficiency of metal oxide reduction to metal. Wang[11] mixed TiO_2 and CaO or CaCO_3 powder and compressed it into sheets to obtain porous

CaTiO₃ cathodes by increasing the porosity through decomposition of CaCO₃. When these CaTiO₃ cathodes are electro-deoxidized in molten CaCl₂, the reduction rate for CaTiO₃ is twice as fast as that for TiO₂, and the current efficiency and energy efficiency are also higher. This is because CaTiO₃ will not react with molten salt, and the 3PI for the porous CaTiO₃ cathode is greater than that for TiO₂. Fray[12] analyzed the effect of varying porosity for TiO₂ cathodes on the reaction process, and the results show that when the porosity of the cathode changes, the process of TiO₂ reduction will also change. The higher the porosity, the faster the reaction process. In practice, however, the preparation of TiO₂ precursors with uniform pores is a difficult and challenging task, and the influence of the pore-forming agent on the efficiency of electro-deoxidation needs in-depth study.

TiO₂ is generally chosen as the precursor for preparing metal titanium by the FFC method, but TiO₂ is an expensive raw material that is produced by the traditional sulfate process, which belongs to the middle and downstream products of the metallurgical process. Although the world is rich in titanium resources, most of them exist in the form of vanadium titanomagnetite. Following the metallurgical process for "steelmaking and vanadium extraction", most of the valuable titanium elements enter the slag. After the fuming process for "selective enrichment, growth and separation", most of the titanium elements in the titanium-containing blast furnace slag turn into CaTiO₃. Compared with TiO₂, CaTiO₃ is easier to obtain and closer to primary minerals[13-15]. Studies have shown that some titanates, such as Na₂Ti₃O₇[16], Ca₃Ti₂O₇, and CaTiO₃[17], have kinetic advantages when molten salt electrodeoxidation is used to prepare metal titanium. In particular, a titanium layer is generated during electrodeoxidation, soluble cations and O²⁻ are released simultaneously, forming a "porous diffusion channel", and the diffusion resistance of O²⁻ is reduced[11,18].

Although CaTiO₃ molten salt electro-deoxidation can be used to prepare titanium metal with more advantages than titanium oxide and the raw materials are easier to obtain[19,20], there are few relevant studies for this process at present, especially studies of key parameters such as sintering temperature and porosity. Improving the deoxidation degree of CaTiO₃ is an urgent problem to be solved in the preparation of titanium metal. In this study, CaTiO₃ was used as a cathode precursor for electrolyzing in molten CaCl₂-NaCl. By controlling the sintering parameters to change the electrical resistivity and improve the electrical conductivity, the effect of sintering temperature on electrical resistivity and the degree of deoxidation was explored. Moreover, by adding NH₄HCO₃ as a pore-forming agent, the influence of porosity on the deoxidation degree was also investigated. The morphology and composition of the electro-deoxidation products were analyzed using XRD, SEM, and EDS.

2. EXPERIMENT

All reagents used in this experiment were analytically pure chemical reagents. A graphite electrode was polished and washed with water and then connected to an electrode wire for use as the anode. CaTiO₃ was used as the cathode, which was formed by pressing CaTiO₃ powder under a pressure of 10 MPa and sintering at 900°C, 1000°C, 1100°C, 1200°C and 1300°C for 4 h to obtain a cathode with high mechanical strength. For the porous CaTiO₃ cathode, 2 wt.%, 4 wt.%, 6 wt.%, 8

wt.% and 10 wt.% NH_4HCO_3 was added to CaTiO_3 powder as a pore-forming agent, mixed evenly, pressed and formed, and then sintered at 1200°C . Both sides of the sintered CaTiO_3 cathode were coated with a 300 mesh iron net of the same size, and then the iron net was wrapped with copper wire to ensure close contact with the cathode surface. The coated cathode was fixed onto the electrode wire with copper wire.

The experimental apparatus used in this work has been reported in our previous work[21]. The molten salt was first pretreated before the experiment. The mixed molten salt with a mass ratio of 7:3 $\text{CaCl}_2\text{-NaCl}$ was dried in an air atmosphere for 48 h and then transferred to an argon atmosphere for further drying for 24 h. When the molten salt was completely melted at 750°C , pre-electrolysis was conducted with two graphite electrodes at 2.5 V for 2 h. Then, another graphite anode and CaTiO_3 cathode were inserted into the molten salt to begin electro-deoxidation at -3.2 V. Graphite crucibles (inner diameter of 80 mm and height of 120 mm) were used as containers for the molten $\text{CaCl}_2\text{-NaCl}$. The whole process of pre-electrolysis and electro-deoxidation was carried out in an argon gas atmosphere, and the change in the current with time was recorded by a computer. At the end of the experiment, the molten salt was removed from the electrode, and argon gas was used to protect the samples until the temperature decreased to room temperature. After being washed with deionized water and anhydrous ethanol, the samples were put into a vacuum drying oven to dry and then stored for subsequent analysis and testing. The samples were characterized by XRD (D8 ADVANCE, Broker AXS, Germany) and SEM (S-4800, Hitachi, Japan).

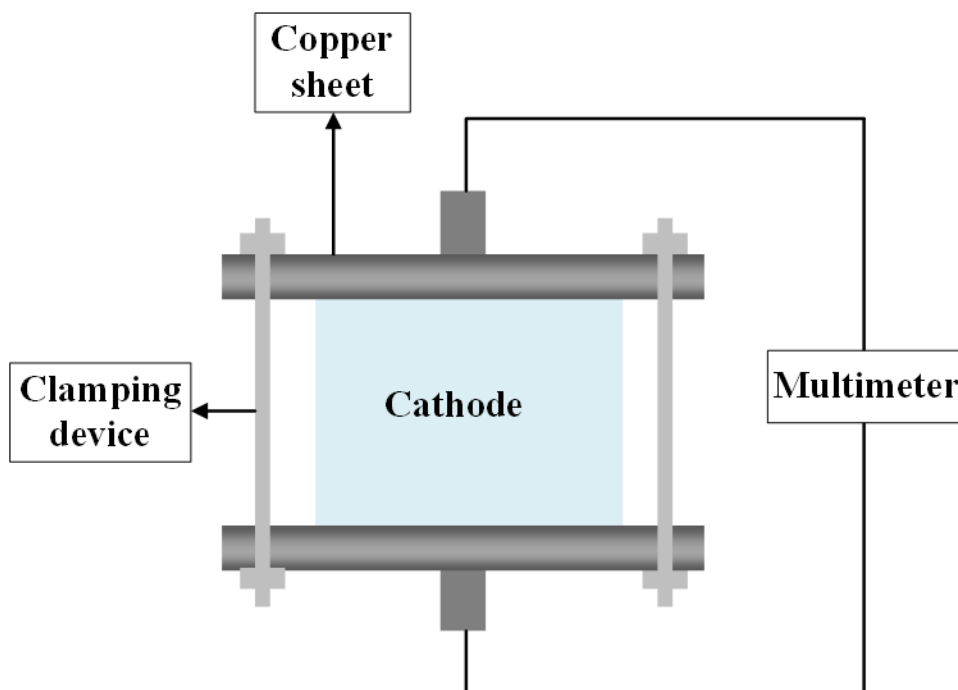


Figure 1. Resistivity measuring device

The cathodic resistivity obtained at different sintering temperatures as measured as follows: First, both sides of the CaTiO_3 cathode were polished smooth with 2000 grit sandpaper, and the upper

and lower sides were clamped with a copper sheet and then fixed with a fixing device. Second, the copper sheet was connected to a wire, and its resistance was measured with a multimeter. The resistivity can be calculated by using Eq. (1).

$$\rho = RS/L \quad (1)$$

where ρ is the resistivity, R is the resistance of the CaTiO_3 cathode, S is the cross-sectional area, and L is the height of the CaTiO_3 cathode.

The device used for measuring cathode resistance is shown in Figure 1.

The porosity (P) of CaTiO_3 cathodes with varying NH_4HCO_3 content was measured by the Archimedes drainage method. Before the experiment, the dry weight (m_0) of the CaTiO_3 cathode was recorded, and then the cathode was placed into a water tank and put under vacuum for 5 min. After water injection, the vacuum was maintained for 5 min, and the suspension weight (m_1) and saturation weight (m_2) of the cathode in the water were determined. The porosity was calculated using Eq. (2).

$$P = (m_2 - m_0)/(m_2 - m_1) * 100\% \quad (2)$$

3. RESULTS AND ANALYSIS

3.1 Effect of sintering temperature on the degree of deoxidation degree of CaTiO_3 in $\text{CaCl}_2\text{-NaCl}$ molten salt

3.1.1 Effect of sintering temperature on the resistivity of the CaTiO_3 cathode

In the electro-deoxidation experiment for CaTiO_3 , electrons are used as reducing agents to reduce CaTiO_3 to titanium; thus, the conductivity of the cathode will affect the degree of electro-deoxidation. However, the sintering temperature has a great influence on the conductivity of the cathode. Table 1 shows the resistivity test results for CaTiO_3 cathodes prepared at different sintering temperatures. It can be seen that with increasing sintering temperature, the cross-sectional area (S) and thickness (L) of the CaTiO_3 cathode after sintering decrease, and the corresponding resistivities (P) also show the same changes. When the temperature rises from 900°C to 1200°C , the resistivity decreases from $2.86 \times 10^6 \Omega \cdot \text{m}$ to $1.16 \times 10^6 \Omega \cdot \text{m}$. Because the resistivity changes little from 1200°C to 1300°C , increasing the sintering temperature has little effect on improving the conductivity of the cathode.

Table 1. Parameters and resistivity of CaTiO_3 cathode sintered at $900^\circ\text{C} \sim 1300^\circ\text{C}$

T($^\circ\text{C}$)	S(m^2)	L(m)	R(Ω)	P($\Omega \cdot \text{m}$)
900°C	174.75×10^{-6}	2.26×10^{-3}	37.03×10^6	2.86×10^6
1000°C	165.05×10^{-6}	2.20×10^{-3}	34.82×10^6	2.61×10^6
1100°C	156.51×10^{-6}	2.16×10^{-3}	26.81×10^6	1.94×10^6
1200°C	137.61×10^{-6}	2.06×10^{-3}	18.80×10^6	1.26×10^6
1300°C	134.85×10^{-6}	1.98×10^{-3}	17.41×10^6	1.16×10^6

The resistivity of the CaTiO₃ cathode depends on the characteristic electrical resistance of the CaTiO₃ particles as well as the contact resistance between the particles[8]. On the one hand, the characteristic electrical resistance of CaTiO₃ particles will decrease with increasing sintering temperature. CaTiO₃ belongs to a ceramic crystal, which should be electrically neutral when forming a defect structure, and it will not appear to have a structure that is similar to oxygen vacancies in oxide crystals alone. A cationic vacation-gap cation (Frankel defect) or cationic vacation-anion vacancy (Schottky defect) defect pair must be present simultaneously. The relationship between the number of these two defect pairs and temperature is shown by Eq. (3) and Eq. (4)[22,23].

$$N_{Fr} = N \exp\left(-\frac{Q_{Fr}}{2kT}\right) \quad (3)$$

$$N_S = N \exp\left(-\frac{Q_S}{2kT}\right) \quad (4)$$

where N_{Fr} and N_S are the numbers of Frankel and Schottky defects, N is the total number of lattice nodes, Q_{Fr} and Q_S is the energy required to form Frankel and Schottky defects, respectively, K is the Boltzmann constant, and T is the thermodynamic temperature.

As the sintering temperature increases, the number of defects in CaTiO₃ increases, then the conductivity of CaTiO₃ particles increases, and, finally, the characteristic resistance of CaTiO₃ particles decreases. However, since CaTiO₃ is a relatively stable crystal, its characteristic resistance does not decrease greatly with changing temperature.

On the other hand, the contact resistance for CaTiO₃ affects the resistivity of the cathode. Thus, the decrease in the resistivity with increasing sintering temperature can also be explained by the compactness of CaTiO₃ particles. When the sintering temperature increases, the liquid phase is generated in the local area of the cathode, which improves the compactness of the cathode structure and increases the connectivity between the particles. The contact area of the CaTiO₃ cathode with good compactness becomes larger, leading to a smaller resistance.

Figure 2 shows the cathode microstructure of CaTiO₃ obtained after sintering at 900~1300°C. Figure 3 shows the equivalent circuit for the cathode as the sintering temperature increases. As shown in Figure 3, the total resistance of the CaTiO₃ cathode includes R_m and R_c . The contact resistance depends on the area of contact between the particles in the cathode cross section. The number of contact points between particles has a great influence on the contact area, and the contact points on the cross section depend on the connectivity between particles. Figure 2 and Figure 3 show that with increasing sintering temperature, small particles in the CaTiO₃ cathode are gradually sintered together to form large particles, and the connectivity between particles is also increased. The cathode particles sintered at 900°C and 1000°C are relatively loose, the particles are mechanically piled together, and the contact area between the particles is small. The contact between particles is similar to a point contact when the total resistance is equal to the sum of R_m and R_{c1} . In this case, the contact resistance is a maximum, and its equivalent circuit is shown in Figure 3(a). The local structure of the CaTiO₃ cathode becomes compact, the contact area between the particles begins to increase, and the contact resistance decreases. At this time, the total resistance is the sum of R_m and R_{c2} , but R_{c2} is smaller than R_{c1} . The equivalent circuit is shown in Figure 3(b). After sintering at 1300°C, the cathode particles are fully sintered together, and the particles move into close contact with each other. At this time, the resistivity

of the cathode is close to the characteristic resistance R_m of CaTiO_3 particles, and its equivalent circuit is shown in Figure 3 (c).

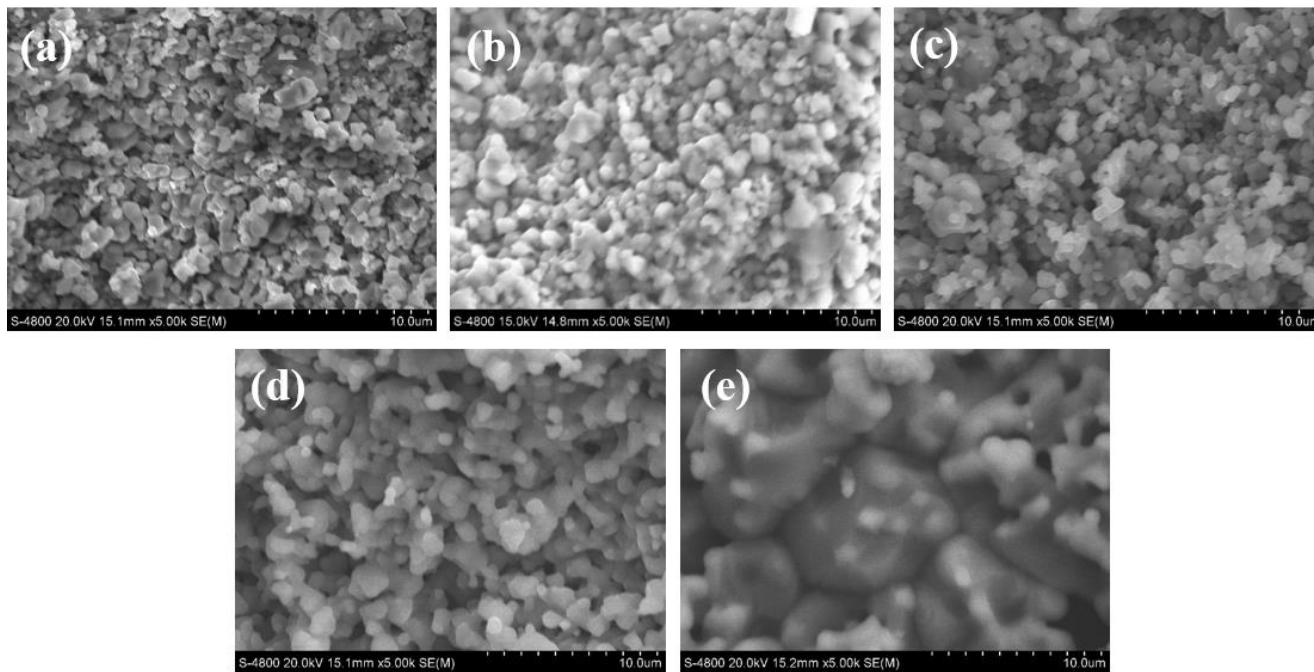


Figure 2. SEM images of CaTiO_3 cathode after 4h sintering at $900^\circ\text{C}\sim 1300^\circ\text{C}$ ((a). 900°C , (b). 1000°C , (c). 1100°C , (d). 1200°C , (e). 1300°C)

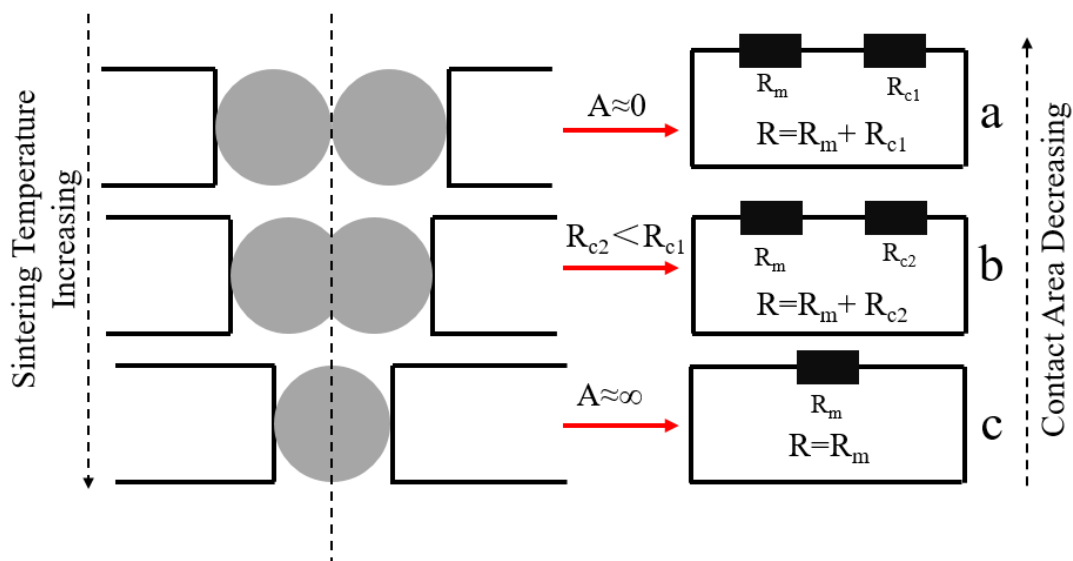


Figure 3. Equivalent circuit of cathode resistance changing with sintering temperature (R_m - CaTiO_3 characteristic resistance, R_c -contact resistance, A -equivalent contact point of CaTiO_3 cathode)

3.1.2 Phase analysis for the electrolysis products at different sintering temperatures

In our unpublished work, the deoxidation process for the CaTiO_3 cathode under 3.2 V in $\text{CaCl}_2\text{-NaCl}$ molten salt was described as follows: $\text{CaTiO}_3 \rightarrow \text{Ti}_2\text{O}_3 \rightarrow \text{TiO}$, $\text{Ti}_2\text{O} \rightarrow \text{Ti}[\text{O}]_6 \rightarrow \text{Ti}$. The reduction process for calcium titanate is divided into four stages. In the first stage, Ca^{2+} and O^{2-} are removed from CaTiO_3 to form Ti_2O_3 . For the second stage, Ti_2O_3 is deoxidized to TiO and a small amount of Ti_2O . In the third stage, TiO and a small amount of Ti_2O continue to deoxidize to form $\text{Ti}[\text{O}]_6$. The fourth stage involves the slow deoxidation of $\text{Ti}[\text{O}]_6$ to titanium metal.

To analyze the effect of sintering temperature on the degree of electro-deoxidation of the CaTiO_3 cathode, the CaTiO_3 cathode sintered at 900~1300°C was subjected to an electrolysis experiment in molten $\text{CaCl}_2\text{-NaCl}$ for the same time. Figure 4 shows the XRD patterns measured for cathodes prepared at different sintering temperatures after electrolysis for 8 h at 3.2 V. As shown in the Figure, the electrolysis product for the cathode sheet sintered at 900°C is mainly CaTiO_3 , and no other phases are produced. No deoxidation occurs at the CaTiO_3 cathode sintered at 900°C because the cathode precursor contains loose particles after sintering, as shown in Figure 2(a). Electrons cannot migrate inside, leading to a failure of the reduction reaction.

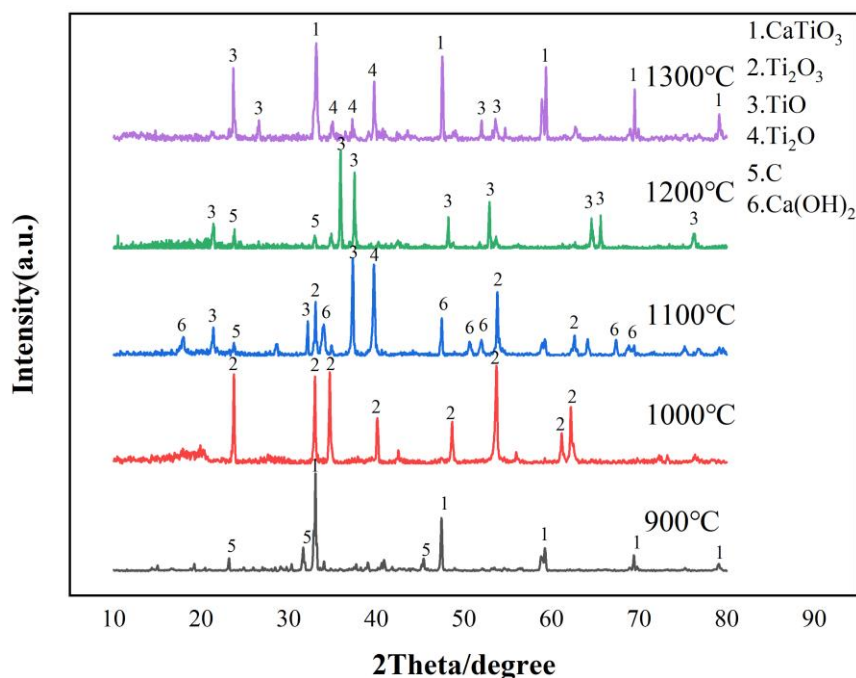


Figure 4. XRD patterns of CaTiO_3 cathode sintered at different temperatures after 8h electrolysis in $\text{CaCl}_2\text{-NaCl}$ molten salt at 750°C

When sintered at 1000°C, the electrolysis product is mainly Ti_2O_3 . This indicates that the cathode sintered at this temperature starts to deoxidize and reaches the first stage of reduction. After electrolysis of the cathode sheet sintered at 1100°C, Ti_2O_3 , TiO and Ti_2O products are formed, and low-price oxides of titanium begin to appear, which indicates that the Ti_2O_3 produced begins to further deoxidize, and that the second stage of reduction has started. The deoxidation of the CaTiO_3 cathode

sintered at 1100°C is deeper than that at 1000°C. The main product of TiO obtained after electrolysis of the CaTiO₃ cathode sintered at 1200°C contains no Ti₂O₃, which indicates that Ti₂O₃ is deoxidized into TiO for the cathode sintered at 1200°C. These are the main products for the second stage when CaTiO₃ is reduced to titanium metal. The CaTiO₃ cathode sintered at 1200°C has a small resistivity and good conductivity, and the electron migration inside the cathode as a reducing agent is less hindered, so the reduction reaction easily occurs. In addition to TiO and Ti₂O, some CaTiO₃ exists in the main products of electrolysis of CaTiO₃ sintered at 1300°C. Although no high-valent oxide of titanium (such as Ti₂O₃) exists, a large amount of CaTiO₃ that has not been reduced is present. Although the resistivity of the CaTiO₃ cathode sintered at 1300°C is small, due to the high sintering temperature and excessive grain growth, and the transmission distance for O²⁻ increases. As a result, the reduction of internal CaTiO₃ is difficult, and the large grain size is not conducive towards deep dissociation reduction of the cathode sheet.

Figure 5 shows the I-t curve for the electrolysis process. As shown in the Figure, with increasing sintering temperature for the CaTiO₃ cathode, the current in the electrolysis process also increases, which is due to the reduced resistivity of the CaTiO₃ cathode. It is worth noting that the cathode sheet sintered at 1300°C can approach a background current at approximately 0.5 h after electrolyzing. Due to the excellent conductivity of the CaTiO₃ cathode sintered at this temperature, the cathode surface becomes a low-priced oxide of titanium. When the activity of oxygen is lower than TiO, O and Ti will combine into a solid solution. Deoxidation from solid solution becomes increasingly controlled by the diffusion of O in Ti. At this point, the solid mass transfer process for oxygen ions inside the cathode becomes the main rate-controlling step for deoxidation, rather than the liquid phase transfer of oxygen ions in the molten salt[24,25]. The process is extremely slow, so the current does not change much at this point.

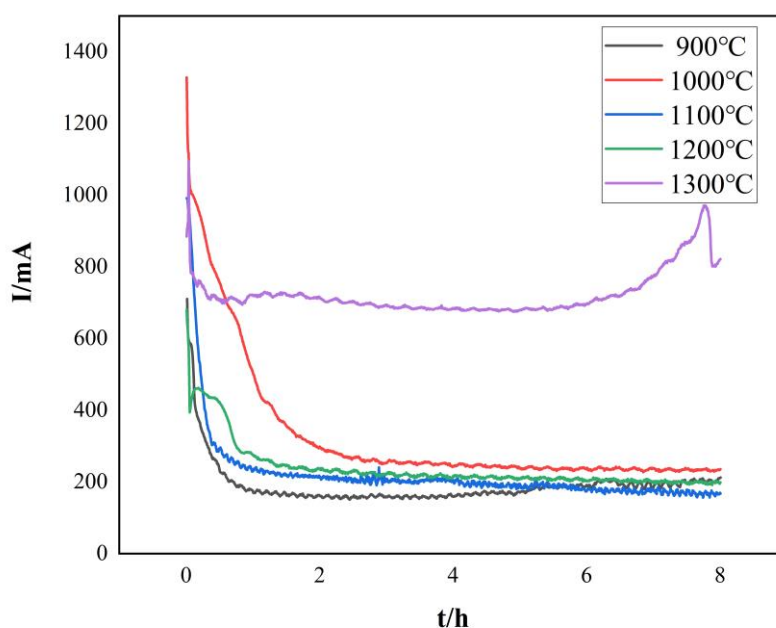


Figure 5. The I-T curve of electrolysis of CaTiO₃ cathodes at different sintering temperatures in CaCl₂-NaCl molten salt at 750°C

However, with time, the distance between the oxygen ion and the solid mass transfer in the cathode becomes longer, which makes the deoxidation process in the cathode difficult. As a result, the surface of the cathode is deoxidized into low-price titanium oxide, but internal deoxidization is difficult, resulting in the inability to carry out deep reduction. When other CaTiO_3 cathodes with good connectivity are reduced to low-price oxides of titanium, due to the network distribution of particles rather than the presence of large particles, as shown in Figure 4(e), oxygen ions can enter the pores. Therefore, the deoxidation reactions for these CaTiO_3 cathodes are jointly controlled by solid mass transfer and liquid phase transport. It is difficult to transfer O^{2-} from cathode to cathode in most of the electrodeoxidation experiments. Shortening the process can greatly improve the speed of the experiment[26].

Combined with Figure 4, it can be seen that there is some impurity C in the electrolysis products. The reason for this is that the CO_2 formed by O^{2-} diffusion to anode C after deoxidization of the CaTiO_3 cathode is not discharged in time, but O^{2-} continues to diffuse to the anode in the molten salt to form CO_3^{2-} . The C cycle mechanism in the electrolysis process is shown in Figure 6. Under the action of the concentration difference between the anode and cathode, CO_3^{2-} starts to diffuse to the cathode. After reaching the cathode, CO_3^{2-} starts to compete with CaTiO_3 for reduction, leaving impurity C in the cathode product. This is also one of the main causes of current loss in the process of electro-deoxidation. This C cycle mechanism generally occurs in the process of electrodeoxidation to prepare metals, such as titanium or chromium, and there will be impurity C in the cathode products[27,28].

Also, $\text{Ca}(\text{OH})_2$ is present in some electrolysis products. When Ca^{2+} and O^{2-} in CaTiO_3 cathode are released into molten salt, CaO will appear in the molten salt electrolyte. CaO are dissolved in $\text{CaCl}_2\text{-NaCl}$ molten salt in ionic state. The presence of NaCl can induce underpotential electrodeposition of CaO , and a small amount of calcium metal can be obtained on the cathode. During sample treatment, Ca react with deionized water to form a small amount of $\text{Ca}(\text{OH})_2$. $\text{Ca}(\text{OH})_2$ is slightly soluble in water. Therefore, there is still a small amount of $\text{Ca}(\text{OH})_2$ in the electrolytic product after washing[29].

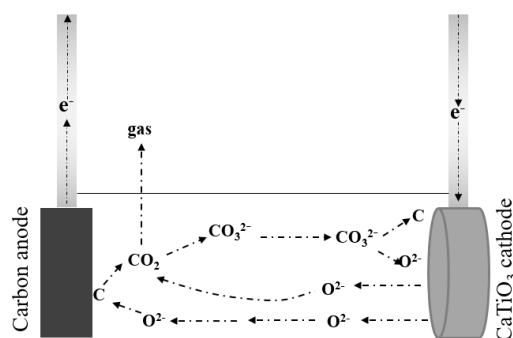


Figure 6. Carbonate cycling mechanism: chemical and cyclic conversion between cathodically discharged, anodically formed, and chemically formed

3.1.3 Morphology of the electrolysis products at different sintering temperatures

Figure 7 shows the morphology of the CaTiO_3 cathode sintered at 900~1300°C after electrolysis for 8 h in $\text{CaCl}_2\text{-NaCl}$ molten salt at -3.2V. Compared with Figure 2, the particles sintered at 900°C grow slightly after electrolysis, and their size is relatively uniform. Some particles take on a certain square shape. However, according to the XRD results, there is basically no change in the phase of the cathode after electrolysis because there are fewer connections between the cathode particles after sintering at this temperature. The internal particles of the CaTiO_3 cathode cannot provide "channels" for electron diffusion, resulting in failure of the electrolysis to proceed normally. The small amount of reduced particles on the surface is easily pulverized due to the extremely low strength of the cathode sheet and is separated from the cathode in the subsequent product processing steps. The composition of the cathode sintered at this temperature does not change significantly before and after electrolysis. After sintering of the CaTiO_3 cathode at 1000 °C, many small particles gather together after electrolysis and gradually form large square particles. This large square particle is formed by the stacking together of many small particles stacked, and the structure of the square particle is relatively loose. Combined with the XRD results, the cathode sheet except the unreacted CaTiO_3 , the main substance present is Ti_2O_3 , so the large square particles are composed of a mixture of Ti_2O_3 and CaTiO_3 . After electrolysis of the CaTiO_3 cathode sintered at 1100°C, the products are mainly Ti_2O_3 and a small amount low-price oxides of titanium and basically contain no CaTiO_3 . The morphology of the products is composed of regular square particles, which are formed by the intermediate products obtained after deoxidization of CaTiO_3 . The product obtained after electrolysis at 1200 °C is mainly TiO , which is formed by the deoxidation of Ti_2O_3 . Its morphology is a long strip, and the degree of deoxidation is deeper than that for the CaTiO_3 sintered at 1100 °C.

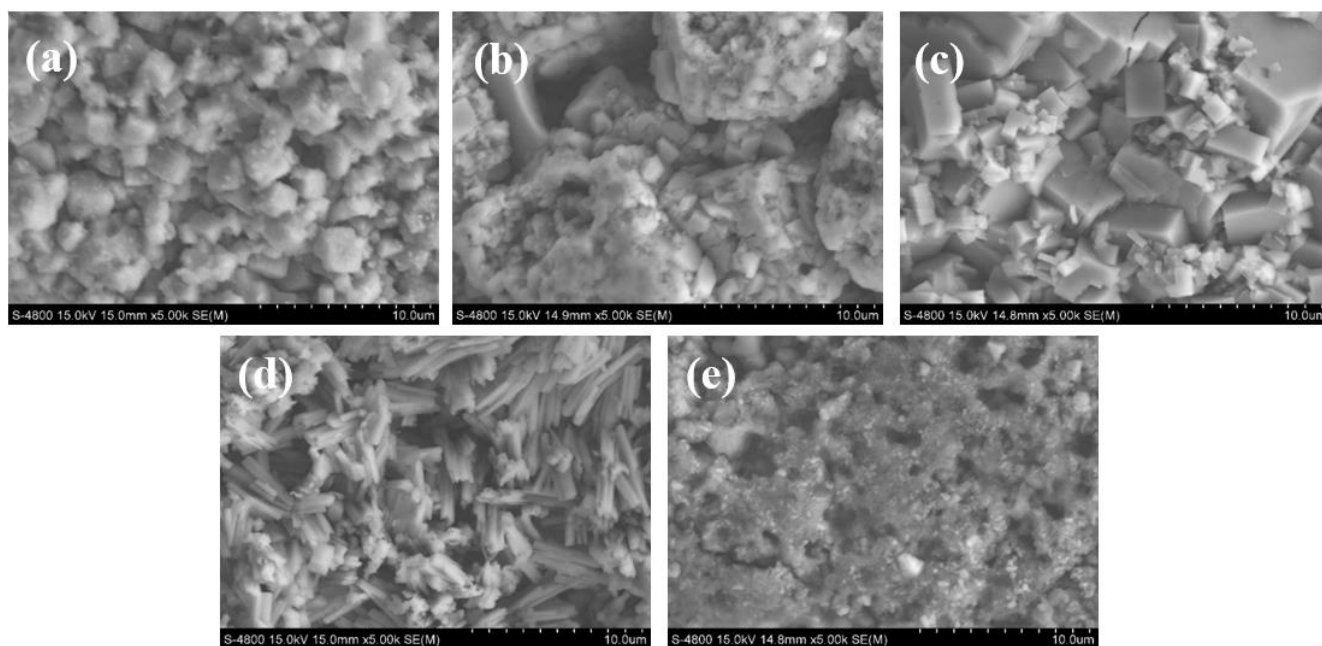


Figure 7. SEM images of CaTiO_3 cathodes at different sintering temperatures after 8h electrolysis in $\text{CaCl}_2\text{-NaCl}$ molten salt at 750°C ((a). 900°C, (b). 1000°C, (c). 1100°C, (d). 1200°C, (e-. 1300°C)

After electrolysis of the CaTiO_3 cathode sintered at 1300°C , some holes appear on the surface of the cathode product. In addition to CaTiO_3 , its cathode product is the low-priced oxide of titanium (TiO , Ti_2O), and no high-priced oxide such as Ti_2O_3 is found to be present. Combined with the XRD test results shown in Figure 2 (e), the sintered cathode surface at this temperature has a compact structure and large grains. Due to the longer solid phase transmission distance of O^{2-} , cathode deoxidation of CaTiO_3 only occurs on the cathode surface, and these holes are generated by the removal of Ca^{2+} and O^{2-} on the surface. CaTiO_3 cathode sintered at $900\sim 1300^\circ\text{C}$ presents different morphologies, such as square, strip and powder, after 8h electrolysis in molten salt. This is because different degrees of deoxidation of CaTiO_3 cathode lead to the formation of different titanium oxides, which have different sintering properties. They show different morphologies after secondary sintering in molten salt[16].

Based on the above analysis, the CaTiO_3 cathode sintered at 1200°C shows the most in-depth deoxidation situation, and this temperature is suitable for electro-deoxidation of the molten salt precursor to prepare titanium.

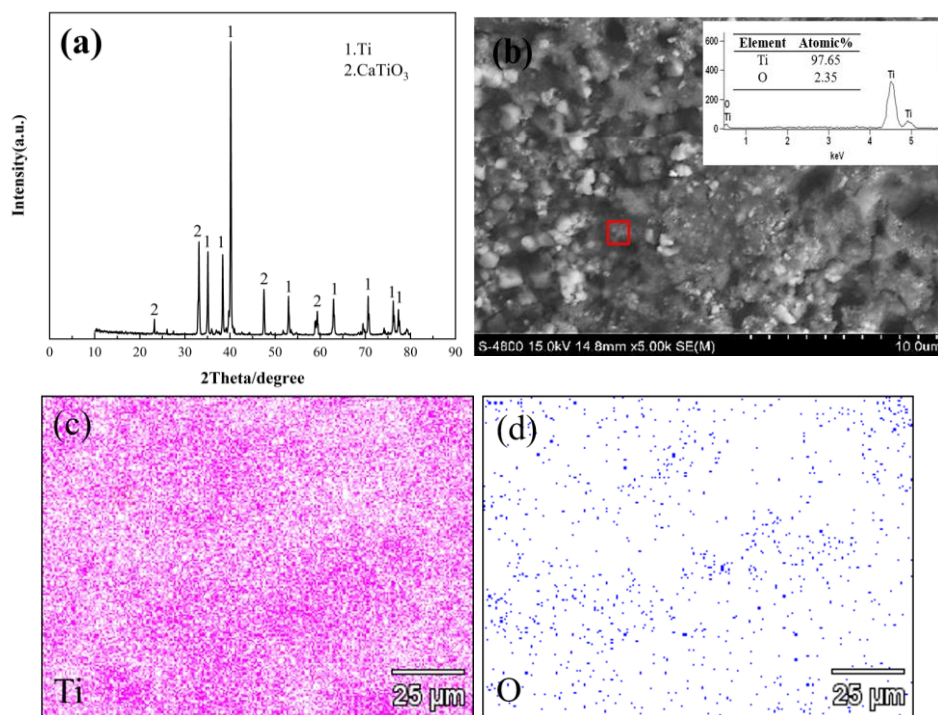


Figure 8. XRD and SEM-EDS analysis of CaTiO_3 cathode sintered at 1200°C for 4h and electrolyzed in $\text{CaCl}_2\text{-NaCl}$ molten salt at 750°C for 24h

From the above results, when the CaTiO_3 cathode sintered at 1200°C was electrolyzed for 8 h, the electrolysis remained incomplete. Then, the electrolysis time was increased to 24 h, and the phase and morphology of the cathode product after electrolysis are shown in Figure 8. As shown in the Figure, the CaTiO_3 cathode is reduced to metal titanium after 24 h of electrolysis, but a small amount of unreacted CaTiO_3 remains behind. Finally, the titanium metal presents a powder morphology, and the purity of the titanium metal was determined to reach 97.65% by energy spectrum analysis.

According to the surface scanning results for the cathode morphology, the element distribution for the CaTiO_3 cathode sintered at 1200°C is more uniform, and the electrolysis is more thorough.

3.2 Effect of porosity on the deoxidation degree of CaTiO_3

3.2.1 Effect of NH_4HCO_3 content on the porosity of the CaTiO_3 cathode

To determine the effect of porosity on the deoxidation of the CaTiO_3 cathode, various NH_4HCO_3 contents were used as pore-forming agents, such as 2 wt.%, 4 wt.%, 6 wt.%, 8 wt.% and 10 wt.%, and added to the CaTiO_3 cathode and sintered at 1200°C for 4 h.

The Gibbs free energy for NH_4HCO_3 at 1200°C is shown in Eq. (5). At the sintering temperature (1200°C), NH_4HCO_3 will automatically volatilize into NH_3 and CO_2 , which are gaseous states that will separate from CaTiO_3 , leaving a gap in the cathode. Table 2 shows the relationship between the amount of NH_4HCO_3 added and the porosity according to Eq. (2).



Table 2. Porosity of CaTiO_3 cathode sintered at 1200°C after adding different contents of NH_4HCO_3

$\text{NH}_4\text{HCO}_3(\text{wt}\%)$	0	2	4	6	8	10
P(%)	24.1	28.6	34.2	39.0	41.4	42.1

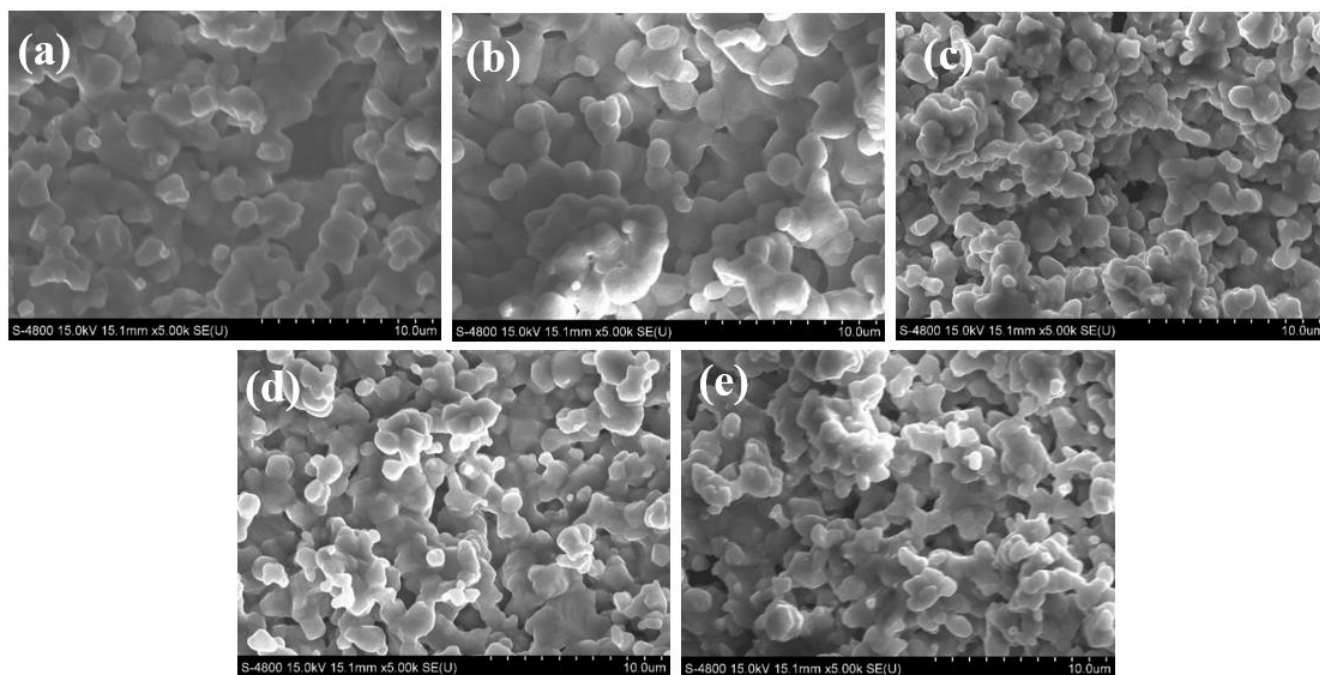


Figure 9. SEM images of CaTiO_3 cathode sintered at 1200°C with different contents of NH_4HCO_3 ((a). 2 wt.%, (b). 4 wt.%, (c). 6 wt.%, (d). 8 wt.%, (e). 10 wt.%)

Figure 9 shows the cathode morphology of CaTiO_3 obtained after sintering at 1200°C for 4h with varying NH_4HCO_3 content. With increasing NH_4HCO_3 content, since NH_4HCO_3 will volatilize into gas in the sintering process, leaving behind pores in the cathode, the cathode gradually becomes loose and porous. With increasing NH_4HCO_3 content, the CaTiO_3 cathode particles gradually become uneven, as shown in Figure 9 (c) and (e), and some of the small particles become stuck together. This is due to the decomposition of NH_4HCO_3 into gas, which promotes small particles to gather together. This behavior will lead to a decrease in the mechanical strength of the CaTiO_3 cathode and an increase in difficulty of operation when connecting the electrode with the cathode wire.

3.2.2 Phase analysis of electrolysis products with varying porosity

Figure 10 shows the XRD patterns measured for cathodes with varying NH_4HCO_3 content after electrolysis for 8 h. After electrolysis of the cathode with high porosity (8 wt.%, 10 wt.% NH_4HCO_3 amount), CaTiO_3 was still obtained as the product. The electrolysis products with 6 wt.% NH_4HCO_3 were composed of a mixture of CaTiO_3 and Ti_2O_3 .

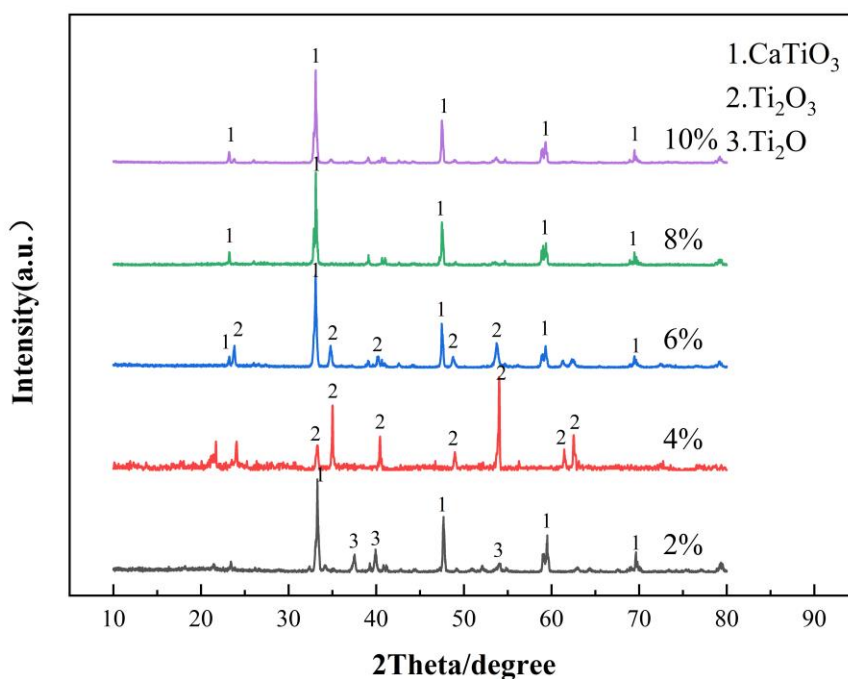


Figure 10. XRD patterns of CaTiO_3 cathodes with different NH_4HCO_3 contents electrolyzed for 8h in $\text{CaCl}_2\text{-NaCl}$ molten salt at 750°C

This indicates that some particles had already started the first stage of reduction. The electrolysis product with 4 wt.% NH_4HCO_3 was Ti_2O_3 , while that with 2 wt.% NH_4HCO_3 was composed of a mixture of CaTiO_3 and Ti_2O . Due to the presence of Ti_2O , its degree of deoxidation was the deepest. Unreacted CaTiO_3 exists in all electrolytic products because with the removal of Ca^{2+} and O^{2-} ions in the CaTiO_3 cathode, the CaTiO_3 cathode will form a porous structure by itself, resulting in a decrease in the mechanical strength of the CaTiO_3 cathode itself and a shedding of some CaTiO_3

particles and cathode matrix. This part of CaTiO_3 does not form a complete loop with the cathode matrix, and electrons cannot reach the particles shedding from the matrix through adjacent particles, leading to failure of the reduction reaction. This is different from the reason for the CaTiO_3 still existing in the cathode electrolysis after sintering at 1300°C .

3.2.3 Morphology of CaTiO_3 cathode with different porosity after electrolysis

Figure 11 shows the morphology of the products obtained after electrolysis with varying amounts of NH_4HCO_3 added. As shown in the Figure, the particle size of the product decreases after electrolysis of the CaTiO_3 cathode with the addition of 2 wt.% NH_4HCO_3 . This is due to the high porosity of the CaTiO_3 cathode after removal of O^{2-} and Ca^{2+} . The low-valent oxide of titanium formed after deoxidation will be broken into such small particles. The CaTiO_3 cathode with 4 wt.% NH_4HCO_3 added is reduced to Ti_2O_3 , and its subsequent deoxidation process becomes difficult. As shown in Figure 11 (b), many large holes are left in the CaTiO_3 cathode due to the removal of O^{2-} and Ca^{2+} on the surface, and the reduction product Ti_2O_3 will undergo spontaneous secondary sintering and gradually aggregate into large particles. The titanium oxide obtained by surface reduction and internal fracture will have gaps, resulting in electro-deoxidation behavior only on the surface.

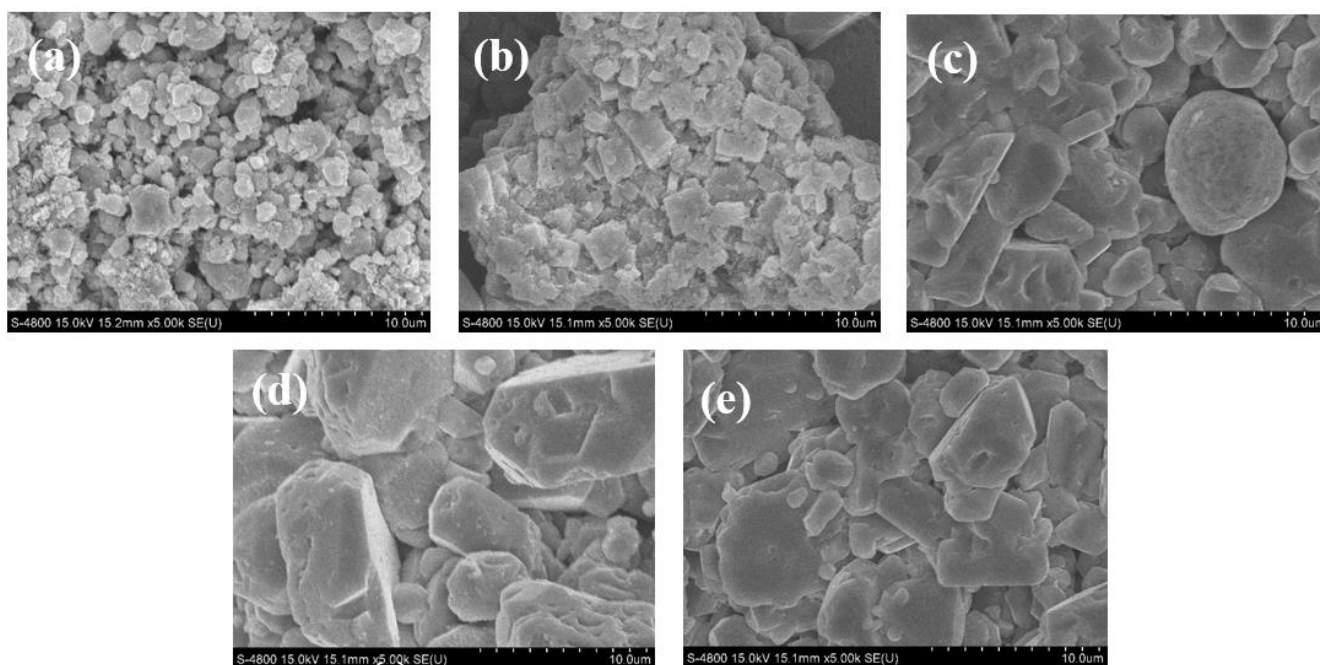


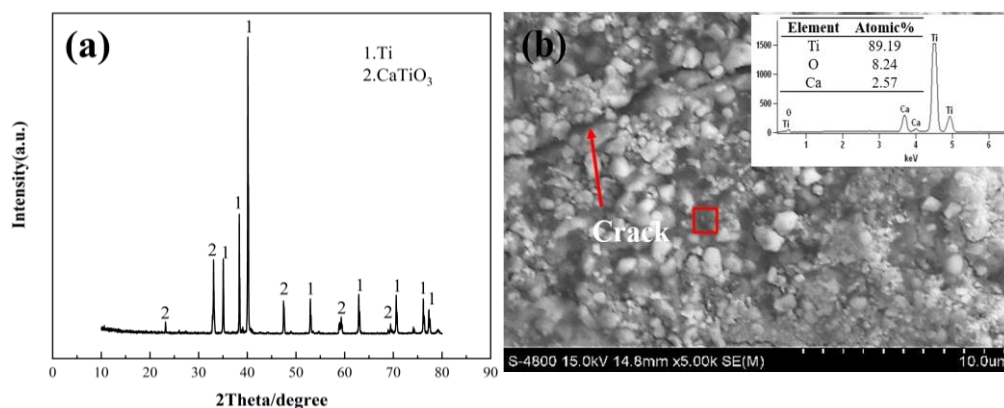
Figure 11. SEM images of CaTiO_3 cathodes with different NH_4HCO_3 contents electrolyzed for 8h in $\text{CaCl}_2\text{-NaCl}$ molten salt at 750°C

The deoxidation behavior of CaTiO_3 cathodes with 6 wt.%, 8 wt.% and 10 wt.% NH_4HCO_3 added only take places on the surface. However, due to the high porosity of these cathodes, the mechanical strength is reduced. In the subsequent processing steps for the products, a small amount of reduced products on the surface fall off the matrix, and then the morphologies of these products differs

from the others. Based on the above analysis, the CaTiO_3 cathode with the addition of 2 wt.% NH_4HCO_3 is the most favorable for electro-deoxidation.

The above result is slightly different from the conclusion obtained by Fray[12] that increasing porosity is favorable for electro-deoxidation. This is mainly because TiO_2 was used as the cathode precursor for electrolysis. TiO_2 interacts with Ca^{2+} in molten CaCl_2 to produce perovskite[11,12] and adds Ca^{2+} to the cathode oxide phase without any oxygen removal, leading to volume expansion of the solid phase, which in turn reduces or eliminates the pore volume in the cathode. As a result, pores for O^{2-} transport in the oxide cathode are partially or fully blocked, resulting in cathodic polarization. Perovskization also occurs at the cathode of other metal oxides, such as chromium (Cr)[28] and Niobium (Nb)[30] oxides. However, the porosity of CaTiO_3 cathode does not decrease during deoxidation. The removal of O^{2-} and Ca^{2+} will only increase the cathode porosity, when CaTiO_3 cathode electro-deoxidation method was used to prepare titanium, the cathode precursor with high porosity is not conducive to deep deoxidation.

To verify whether or not adding NH_4HCO_3 is beneficial to the deoxidation of CaTiO_3 , an electrolysis experiment was carried out for the porous cathode after adding 2 wt.% NH_4HCO_3 under the best deoxidation conditions (sintering at 1200°C , electrolysis time of 24 h and voltage of 3.2V. Figure 12 shows the XRD and SEM-EDS analyses for the cathode product after electrolysis. The products are mainly titanium metal and CaTiO_3 . According to the EDS analysis results, the calcium content is 2.57%, and the purity of the titanium can reach 97.71%, which is not much different from the purity of titanium obtained from the CaTiO_3 cathode without NH_4HCO_3 . According to the surface scanning results for the cathode morphology, the element distribution for the CaTiO_3 cathode with the addition of 2 wt.% NH_4HCO_3 is uneven, and the electrolysis is incomplete. Some unreacted CaTiO_3 exists in the cathode product because the cathode with high porosity will produce cracks in the electrolysis process, as shown in Figure 12(b). These cracks hinder electron migration, leading to an "open circuit" in a part of the cathode, and then the cathode is not completely reduced. Therefore, CaTiO_3 cathode with high porosity is not conducive to electro-deoxidation, which is the same conclusion reached by Li[31] when using a MgO-ZrO_2 precursor system to prepare a Mg-Zr alloy.



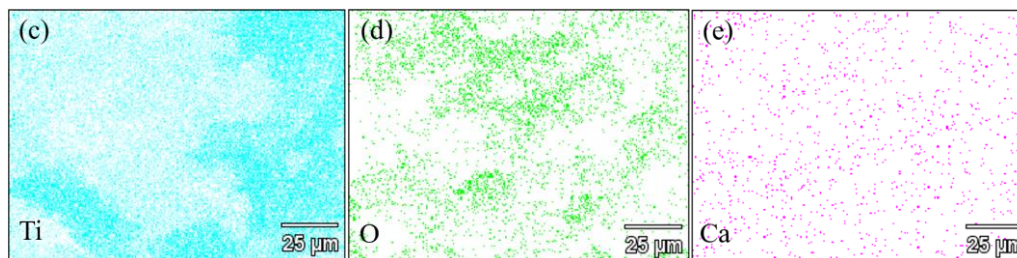


Figure 12. XRD and SEM-EDS analysis of CaTiO_3 cathode with 2 wt.% NH_4HCO_3 content after 24h electrolysis in CaCl_2 - NaCl molten salt at 750°C

The electro-deoxidation of the CaTiO_3 cathode in the CaCl_2 - NaCl molten salt is jointly controlled by electron migration, O^{2-} solid phase transport and liquid phase transport. The sintering temperature mainly affects the conductivity, and the better the conductivity, the easier the electron migration. However, if the sintering temperature is increased, the conductivity will become better, and the grain size will become overgrown, resulting in a larger particle size and longer transmission distance for the O^{2-} solid phase, which is not conducive to deep dissociation and reduction. By increasing the porosity, the molten salt can enter the cathode. O^{2-} only needs to pass through a small solid phase transfer to enter the molten salt and begin to transfer to the liquid phase of the anode. However, the CaTiO_3 cathode will automatically form a porous structure in the electrolysis process. If the porosity increases, the mechanical strength of the cathode will reduce, cracks will be generated in the electrolysis process, and the cathode is no longer a monolithic entity that allows electrons to migrate freely. Deoxidation will only occur in part of the cathode, which is not conducive to deep dissociation and reduction.

4. CONCLUSION

The electro-deoxidation of CaTiO_3 was conducted in molten CaCl_2 - NaCl at 750°C under 3.2 V, and the effect of sintering temperature and porosity on electro-deoxidation was studied. The electro-deoxidation results obtained for a CaTiO_3 cathode sintered at $900\sim 1300^\circ\text{C}$ show that 1200°C is the best sintering temperature. After 24 h of electrolysis, titanium was obtained as the reduction product by sintering at 1200°C , with a purity reaching 97.65%. With increasing sintering temperature, the resistivity of the CaTiO_3 cathode decreases. Increasing the porosity of the cathode can shorten the transport distance for the O^{2-} solid phase and enable liquid phase transport to begin as soon as possible. However, the porosity is not as high as it could be, and the CaTiO_3 cathode forms a porous structure with the removal of O^{2-} and Ca^{2+} . Excessively high porosity leads to crack regions in the electrolysis process for the CaTiO_3 cathode, where electrons cannot be transferred and deoxidation cannot be carried out continuously. As a result, some of the CaTiO_3 exists in the cathode products. By studying the influence of the pore-forming agent content on the deoxidation effect, it is found that when 2 wt.% NH_4HCO_3 of pore former is added, the porosity is 28.6%, and some unreacted CaTiO_3 is present in the cathode product after 24 h of electrolysis, and the purity of the obtained titanium metal is 97.71%, which is similar to that found for the electrolysis of CaTiO_3 without NH_4HCO_3 . In general, the most

suitable precursor for the preparation of titanium at a sintering temperature of 1200°C is a CaTiO₃ cathode without NH₄HCO₃, which enables Ti metal to be prepared successfully. This approach provides a new method for the efficient and sustainable electrolytic reduction of titanates.

COMPETING INTERESTS

The author(s) declared no potential conflicts of interest with respect to the research, authorship, and/or publication of this article.

ACKNOWLEDGMENTS

The authors acknowledge the National Science Foundation of China (Grant No. 51804124), Hebei Natural Science Foundation of China (Grant No. E2020209097) and Science and technology project of Tangshan City (21130229C). We would like to thank AJE (www.aje.com) for English language editing.

References

1. G.Z. Chen, D. J. Fray and T.W. Farthing, *Nature*, 407(2000)361.
2. G.Z. Chen, E. Gordo, D.J. Fray, *Metall. Mater. Trans. B.*, 35(2004)223.
3. K.T. Kilby, S. Jiao and D.J. Fray, *Electrochim. Acta*, 55(2010)7126.
4. R. Barnett, K.T. Kilby and D.J. Fray, *Metall. Mater. Trans. B.*, 40(2009)150.
5. V. Kaplan, E. Wachtel and I. Lubomirsky, *J. Electrochem. Soc.*, 159 (2012) E159.
6. C. Schwandt, G.R. Doughty and D J Fray, *Trans Tech Publications Ltd.*, 436(2010)13-25.
7. S. Jiao, D.J. Fray, *Metall. Mater. Trans. B.*, 41 (2010)74.
8. X.Y. Liu , M.L. Hu, C.G. Bai and X.W. Lv, *Rare Met. Mater. Eng.*, 46(2017)1176.
9. O.Y. Kurapova, A.G. Glukharev, O.V. Glumovl and V.G. Konakov, *Open Ceram.*, 5(2021)100086.
10. W. Li, X.B. Jin, F.L. Huang and G.Z. Chen, *Angew. Chem. Int. Ed.* 122 (2010)3271.
11. K. Jiang, X.H. Hu, M. Ma, D.H. Wang, G.H. Qiu, X.B. Jin and G.Z. Chen, *Angew. Chem. Int. Ed.*, 45(2006)428.
12. C. Schwandt, D.J. Fray, *Electrochim. Acta*, 51(2005)66.
13. Z.T. Sui, P.X. Zhang, C. Yamauchi, *Acta Mater.*, 47(1999)1337.
14. J.Q. Han, J Zhang, J.H. Zhang, X. Chen, L. Zhang and G.F. Tu, *Hydrometallurgy*, 201(2021)105577.
15. Y. Du, J.T. Gao, X. Lan and G.C. Guo, *Ceram. Int.*, 46(2020)9885.
16. K.J. Liu, Y.W. Wang, Y.Z. Di and J.P. Peng, *Electrochim. Acta*, 318(2019)236.
17. D. Wang, S. Pang, C.Y. Zhou, Y. Peng, Z. Wang and X.Z. Gong, *Int. J. Miner. Metall. Mater.*, 27(2020)1618.
18. A.M. Abdelkader, K.T. Kilby and A. Cox, *Chem. Rev.*, 113(2013)2863.
19. M.Z. Wu, H.H. Lu, M.C. Liu, Z.L. Zhang, X.R. Wu, W.M. Liu, P. Wang and L.S. Li, *Hydrometallurgy*, 167(2017)8.
20. G.Q. Fan, M. Wang, J. Dang, R. Zhang, Z.P. Lv, W.C. He and X.W. Lv, *Waste Manage*, 120(2021)626.
21. Y.Q. Cai, X.G. Chen, Q. Xu and Y. Xu, *R. Soc. Open Sci.*, 6(2019)181278.
22. G.C. Mather, M.S. Islam and F.M. Figueiredo, *Adv. Funct. Mater.*, 17(2007)905.
23. L.Y. Li, D Zhang, J.C. Liu and Y.G. Li, *Mater. Res. Express*, 6(2020)125210.
24. C. Schwandt, *Electrochim. Acta*, 280(2018)114.
25. Y. Peng, D. Wang, Z. Wang, X.Z. Gong, M.Y. Wang, T. Qi and F.C. Meng, *J. Alloys Compd.*, 738(2018)345.
26. C. Osarinmwian, I.M. Mellor and E.P.L. Roberts, *Electrochim. Acta*, 209(2016)95.

27. G.Z. Chen, *Int. J. Miner. Metall. Mater.*, 27(2020)1572.
28. E. Gordo, G.Z. Chen and D.J. Fray, *Electrochim. Acta*, 49(2004)2195.
29. S.L. Wang, W. Wei, S.C. Li and S.H. Cao, *Int. J. Miner. Metall. Mater.*, 17(2010)791.
30. T. Wu, W. Xiao, C. Liu, D.H. Wang and G.Z. Chen, *Phys. Chem. Chem. Phys.*, 10(2008)1809.
31. N. Li, Y.R. Peng, W.J. Xiong, J.Q. Sun, Y.M. Chen, P.T. Zhang, M.Y. Liu and S.J. Li, *Electrochim. Acta*, 372(2021)137816.

© 2022 The Authors. Published by ESG (www.electrochemsci.org). This article is an open access article distributed under the terms and conditions of the Creative Commons Attribution license (<http://creativecommons.org/licenses/by/4.0/>).